ISSN: 0975-8585

Research Journal of Pharmaceutical, Biological and Chemical Sciences

Active Factors of Low Ionised Plasma Radiation Produced in Air Spark Discharge.

Igor M. Piskarev*

Skobeltsyn Institute of Nuclear Physics, Lomonosov Moscow State University, 1(2), Leninskie Gory, Russian Federation, 119234.

ABSTRACT

The chemical activity for pulse radiation low ionised plasma of air spark electric discharge was investigated. The power discharge pulse was 0.059 J, pulse repetition frequency 10 Hz, and current pulse duration 150 μs. The energy, released in the discharge gap in the time of current pulse is less than the energy, which needs to ionise nitrogen and oxygen. Therefore the active species in the discharge region itself is not produced. The only active factor of discharge is plasma radiation. Pulse radiation UVC range generates in water the primary active species: radicals $HO_2^{\bullet}$, $O^{\bullet}$ and molecules N_2O. Under pulse radiation in water, a strong acidity effect is created. With the continuous UVC radiation of a mercury lamp having a photon flux 430 times more than the pulse discharge radiation, the acidity effect in water is not produced. Secondary active species are nitrous and nitric acid, peroxinitrite and peroxinitrous acid. Peroxinitrite and peroxinitrous acid formed complex produced under the pulse radiation, during the decay of which in water chemical activity was retained for up to 14 days. The concentration of peroxinitrite/peroxinitrous acid produced in the water sample is about 10^{-3} mol/l.

Keywords: low ionised plasma radiation, pulse discharge, peroxinitrous acid, long-living complex

Highlights

- Low ionised plasma pulse radiation.
- Primary species produced under pulse plasma radiation in water are: $HO_2^{\bullet}$, $O^{\bullet}$, N_2O.
- Secondary species are: $ONOOH/ONOO^{-}$, NO_2^{-}, NO_3^{-}.
- The final species are NO_3^{-} ions.
- Production of a complex, which decays over 14 days, is identified.

Corresponding author

ISSN: 0975-8585

INTRODUCTION

The mechanisms of chemical and biological effects of UV-radiation on liquids are well established. There are valuable reviews concerning these topics [1, 2]. Under UV radiation, direct absorption of photon energy leads to excitation of molecules with biological object destruction (DNA molecule), and the chemical effect of light through reaction with initiators (type 1 and type 2 reactions) [3]. A water molecule has no strong energy levels in the range 200–800 nm: therefore there are no chemical transformations in pure water, owing to the absorption of light energy by water molecules.

In contrast to light radiation, particles of strong ionised plasma entering water initiate chemical reactions between active species and compounds dissolved in water [4]. The strength of the electric field in the electric discharge region is high, and the plasma itself is hot: direct contact of plasma with treated object causes heat damage. The average temperature of the plasma in the discharge region is about 10^5 K, which corresponds to the average energy of the molecules in the discharge E = (3/2) kT ~ 13 eV. The ionisation energy of oxygen and nitrogen molecules is 13–14 eV, so in this region of the discharge, the high temperature provides the highly ionised plasma, which produces a wide range of active species (i.e. radicals and excited molecules). For direct impact on biological objects, cold plasma is used. One method of generating a cold plasma, not producing thermal damage to the object, is a gliding arc. The primary active particles are formed in the discharge region. The discharge region is blown off by wet gas (air), in which a secondary active species is produced. Active species are delivered by means of a gas stream to the surface of the treated object. The strong acidity effect has been found in pure water under a gliding arc [5]. The energy concentration in the gliding arc is sufficient to create all known active species. The thermal radiation spectrum of highly ionised plasma is in the region of vacuum ultraviolet, being strongly absorbed by air, and not passing through the air; therefore, the radiation of highly ionised plasma does not play an essential role.

Photons of the UVC range have essentially less energy than highly ionised plasma particles. However, the creation of active species (radicals) in water under UVC radiation is energetically possible. The part of UVC radiation in chemical effects of plasma is strongly increased, when the electric field strength in the discharge gas is decreased, and becomes decisive for low ionised plasma [6]. The probability of active species (radicals) being generated in low ionised plasma is very small, and the chemical effects of low ionised plasma itself are insignificant. During direct contact of low ionised plasma with biological objects, it can produce only heat damage. The plasma temperature of electric spark discharge in [6] was chosen as about 1.2×10^4 K. The average energy of gas molecules for that discharge is ~1.5 eV, which does not allow gas ionisation, nor the generation of an active species (radicals). The maximum of the radiation spectrum of such a plasma is at wavelength ~220 nm, and almous all radiation energy hits the treated object. The probability of radical creation in water is strongly increased when pulse radiation is used [6]. The continuous spectrum of UVC radiation has some advantages in biophysical research compared to monochromatic line, as it allows vital cell structures to be affected: nucleic acids, proteins and membranes, the absorption lines of which are in various parts of the UVC range. Therefore, the continuous radiation spectrum, in contrast to monochromatic lines, provides multichannel destructive action on an object. In all cases, the nonlinear dependence of yields of processes is possible, depending on the intensity of the radiation.

The goal of the work is a detailed analysis of processes in water under a pulse UVC air spark discharge radiation of low ionised plasma, and a comparison with continuous UVC radiation of a low-pressure mercury lamp.

MATERIALS AND METHODS

The source of pulse UVC radiation was air-discharged spark plasma. The scheme of the discharge circuit is shown in Fig. 1a. The capacitor C was charged through the ballast resistor R = 10 MΩ from a high voltage power supply U = 11 kV. The capacitor C was connected to the discharged electrodes by means of an aluminum bus 5 mm in thickness. The stainless steel electrodes 2 mm in diameter had a total length of not more than 15 mm. The discharge gap was chosen as 3 mm to provide a breakup voltage of 6 kV. When high voltage switches were on, the self-supporting spark discharge started. The pulse repetition rate was determined by the RC value. The flux of UVC photons was determined by means of a ferro oxalate dosimeter. Measurement results are shown in Table 1. A view of the radiation module is shown in Fig. 1b.

ISSN: 0975-8585

Table 1: Yields of active species in water under pulse low ionised plasma radiation of air spark discharge and continuous radiation of a mercury low-pressure lamp.

Active particle	Spark discharge	Mercury lamp
Flux UVC photons	$(1.26\pm0.2) \times 10^{-10}$ mol$(cm^2\ s)^{-1}$ [6]	5.4×10^{-8} mol$(cm^2\ s)^{-1}$ *)
Pulse photon flux	$(1.2\pm0.2) \times 10^{-7}$ mol$(cm^2\ s)^{-1}$ [6]	-
$HO_2^{\bullet}$	$(1.2 \pm 0.3) \times 10^{-6}$ mol$(l\ s)^{-1}$	$(1.1\pm0.5) \times 10^{-6}$ mol$(l\ s)^{-1}$
$NO_2^- + NO_3^-$	$(5.8 \pm 1.6) \times 10^{-7}$ mol$(l\ s)^{-1}$	$< 3.4 \times 10^{-9}$ mol$(l\ s)^{-1}$
NH_4^+	$(1.7\pm0.5) \times 10^{-10}$ mol$(l\ s)^{-1}$	$(2.5\pm1.5) \times 10^{-8}$ mol$(l\ s)^{-1}$
O_3	$< 10^{-5}$ mol/l	$< 10^{-5}$ mol/l
$OH^{\bullet}$	$< 10^{-8}$ mol/l	$< 10^{-8}$ mol/l
H_2O_2	$< 5 \times 10^{-5}$ mol/l	$< 5 \times 10^{-5}$ mol/l
Complex (ONOOH…$ONOO^-$)	$(2.5 \pm 0.5) \times 10^{-3}$ mol/l.	-
*) Technical manual		

The source of continuous UVC radiation was the low-pressure mercury lamp DBK-9 (Russia). The power of the lamp was 9 J/s (W); the radiation wavelength was 253.7 nm, and the density of energy flux at a distance 3 cm from the lamp was $2.6\ 10^{-2}$ J$(cm^2\ s)^{-1}$ according to technical reference manual.

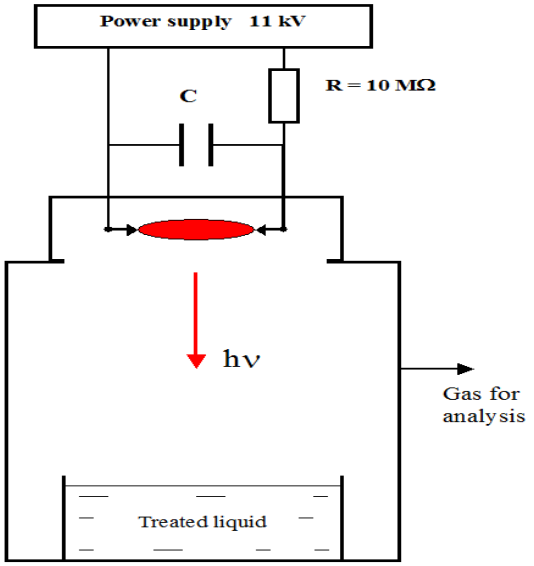

Figure 1a. Plasma radiation source and treatment setup.

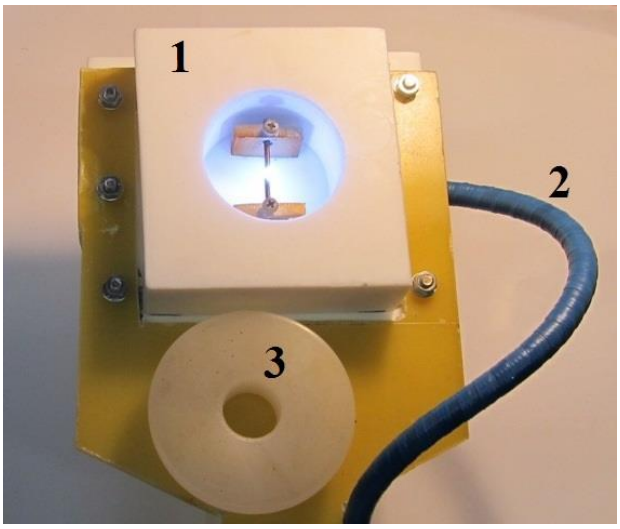

Figure 1b. View of radiation source at time of discharge. 1) discharge module; 2) high voltage cable; 3) additional header. There is no gas flow from the discharge region to the treated liquid surface.

ISSN: 0975-8585

Samples of water were treated to both radiation sources in the same glass vessel. The diameters of the vessels used were 90 mm and 120 mm, volume 0.6 l (see Fig. 1a). The radiation source, spark discharge module or mercury lamp, was mounted on the top of the vessel. The Petri dish was 90 mm in diameter and 45 ml in volume, and was placed on the bottom of vessel. A support to the dish was used to provide necessary distance from the radiation source to the liquid surface. The water was poured into vessel itself, if a large volume of liquid were needed. The distance between radiation sources of both types and the water surface in all cases was 30–60 mm. In the wall of the vessel was a hole to take gas samples. The concentration of ozone in the gas samples was measured by means of chemiluminescent ozone analyzer 3-02.P-R (Russia, St. Petersburg) with sensitivity 1 μg/m^3. The samples of gas were evacuated from the reaction vessel and blown through 5% KI solution to evaluate an oxidant concentration, which could be produced in the vessel under spark discharge. The blow rate was 0.5 l/min. The evaluation of active products (species) was made by means of chemical methods, which are described in each experiment.

The concentration of radicals was evaluated by means of 0.02 N aqueous solution of oxalic acid and 0.01 N Mohr's salt solution in sulphuric acid (pH = 2). The concentration of oxalic acid and Mohr's salt before and after treatment was determined by titration with potassium permanganate 0.05 N at temperature 80 °C.

The concentration of oxidants in the treated water was determined iodometrically: in the water sample, 45 ml was added to 5 ml 5% solution KI and 5 ml 2N sulphuric acid. The concentration of released iodine was determined by titration with 0.02 N sodium thiosulphate. The Nessler reagent determined the concentration of NH_4^+ ions.

UV absorption spectra of the treated aqueous solutions were measured by device Fluorat-02 Panorama (Lumex Firm, Russia, St. Petersburg). IR absorption spectra were measured by IR-Fourier spectrometer FSM 1202 (Russia, St. Petersburg). The pH was measured using the device Expert-001 (Ekonics Firm, Russia, Moscow). The concentration of NO_3^- and NO_2^- ions was determined by ion-selective electrodes EM-NO3-1 and EM-NO2-1 (Firm Analitpribor, Georgia, Tbilisi). We used chemically pure reagents, distilled pH = 5.3 and double distilled water pH = 6.5.

EXPERIMENTAL RESULTS

Stages of electric discharge

The dependence of voltage on the discharge gap at the time of discharge for value C = 3.3 nF is shown in Fig. 2. The discharge arises at high voltage on the discharge gap of about 6 kV. The first stage is streamer discharge, at which time in the discharge gap there is a high-strength electric field. After 50 ns, the voltage falls by approximately a factor of two, for 0.1 μs voltage falls to 1 kV. After 1 μs, the discharge becomes an arc, and the voltage on discharge gap is 100–200 V. After ~150 μs capacitor C is discharged, the discharge stops, and the voltage across the discharge gap begins to grow slowly. After reaching the breakdown voltage the process is repeated. Thus, the duration of the leading edge of radiation pulse was ~ 50 ns, the total pulse duration of ~150 μs at C = 3.3 nF. The phases of the electric discharge can be divided into two stages.

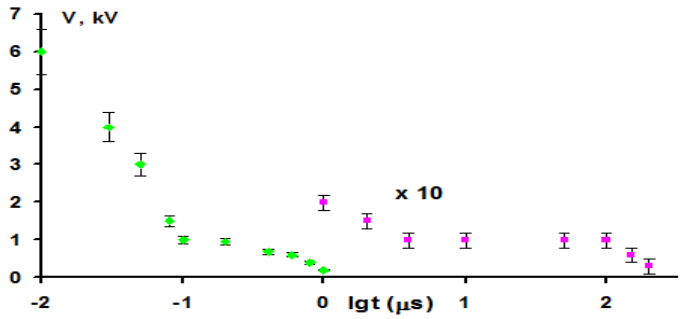

Figure 2. Voltage on discharge gap in time of one pulse self-supporting discharge at C = 3.3 nF. The time starts with the appearance of the discharge current. At the end of the pulse by ~150 μs after the discharge starts, the voltage applied to discharge gap slowly (at the time ~100 ms) increases at the level of the breakdown (~ 6 kV). Self-supporting discharge occurs with a frequency of 10 Hz.

1) Leading edge of discharge (50–100 ns). At this time, the electric field in the gap between the electrodes is a maximum. The potential difference between the electrodes is about 6 kV. At this stage, the probability creation of exited species (radicals) is high.

2) Establishment of a regime of arc discharge and main pulse current duration (100 ns – 150 μs). At the stage of arc discharge, a spark channel is heated conductor. The potential difference between electrodes falls by up to 100–200 V. The strength of the electric field in the discharge channel is minimal. The active species produced during first stage are terminated in interactions between themselves. The entrainment of active species from the discharge region does not occur, as there is no gas blown through this region. Therefore, in the first stage, the spark channel is the source of reactive species; part of them is terminated immediately on the spot formation, while others – on the second stages of discharge. In the second stage, the discharge is a source of UV radiation of the heated black body. The discharge terminates all active species formed in the first stage. New active species are not produced, as the temperature of the plasma cord is not sufficient to ionise gas molecules. From the active species produced earlier, stable products are formed. In between the discharge pulses, long-lived products, arising on the second stage, diffuse within the vessel in which the sample of water is treated. Therefore, the main factor of low ionised plasma in our case is the radiation of heated gas, as products, diffusing from the discharge region, are inactive, and active species, produced during a very short time of the first stage, are terminated on the spot formation.

Selecting conditions spark electric discharge

The pulse spark discharge radiation of low ionised plasma produces in treated water some chemical effect. The main chemical effect under plasma radiation of spark discharge is to reduce the pH [6]. Active species, produced in water, at too high a concentration can be terminated with each other, without producing the chemical effect [7]. Therefore, there is an optimal electric discharge power at which the chemical effect in the water is maximised. The power of discharge for a given length of discharge cord and gap voltage value to which the capacitor is charged is determined by value of capacitance C.

Therefore, we investigate the dependence of the pH water sample volume of 40 ml after treatment with plasma radiation from the capacitance C. The value of high voltage was 11 kV. Treatment time was 10 min. If we change the C, the pulse repetition frequency changes as well. The average current consumed from the power supply did not change and amounted to 0.5 mA. The power released in the spark gap remained constant. The dependence of pH ~ f(C) is shown in Fig. 3. It is evident that the greatest reduction in pH is observed when C = 3.3 nF (pH = 3.07 ± 0.02). As with decreasing and increasing discharge capacity C, the pH value after treatment is increased, while the chemical effect decreases for non-optimal values of C.

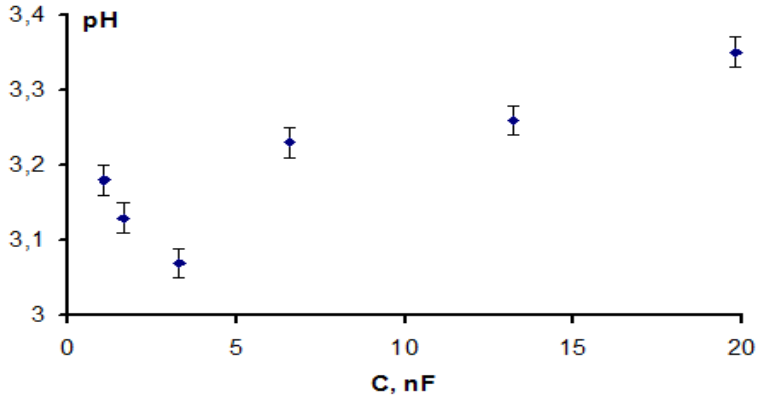

Figure 3. Dependence of pH for water sample of 40 ml volume after treatment to low ionised plasma radiation of pulse electric discharge during 10 minutes from discharge capacitor value C (nF). Supply voltage was 11 kV; the average current consumption from the power source for each value of C is 0.5 mA.

A decrease in C (less than optimal value) leads to the discharge power and the radiation flux decreasing. The number of species generated in the liquid also decreases. With a decrease in capacity less than the optimal value, the pulse energy is decreased, the temperature of plasma is decreased, and the spectral

maximum is shifted toward longer wavelengths, the chemical activity of which is weaker. Therefore there are two factors that determine the decreasing of chemical effect with decreasing capacitance values to less than optimal.

With increasing C to a more optimal value, the discharge power increases, and the probability of active species termination in the interactions between them also increases. A large portion of the active species generated by the radiation in liquid terminates without producing a chemical effect. The second factor, leading to a reduction of the chemical effect with increasing power of electric discharge, is a shift in the spectrum of the heated discharge cord into the vacuum ultraviolet region. Air absorbs part of radiation energy. After shifting, a share of the energy lost by absorption in the air increases with increasing discharge power. Therefore, there are also two factors that determine the decreasing of chemical effect with increasing capacitance values to more than optimal.

As the cooling of the spark cord after discharge ends, the maximum of the radiation spectrum is shifted toward longer wavelengths, and travels through the entire area of UVC radiation spectrum (200–280 nm), causing chemical and biological effects. With increasing wavelength (over 280 nm), the chemical effects are greatly reduced, and changes in pH of the treated water do not take place (see data for mercury lamp).

Evaluation of electric discharge plasma characteristics

Let us now evaluate spectral characteristic radiation of the heated black body. For this purpose, we consider the relation between energy in plasma cord and plasma temperature. Let η be the coefficient of efficiency electrical energy transformation to heat, $W_0 = \frac{CU^2}{2}$ energy capacitor charge. Then:

$$\eta W_0 = mc_v \cdot \Delta T = \rho \cdot \pi \cdot r^2 \cdot \ell \cdot c_v \cdot \Delta T \qquad (1)$$

Where ρ=1.29 10^{-3} g/cm^3 — air density; r — radius of plasma cord; ℓ — length of discharge gap; c_v=0.72 J g^{-1} K^{-1} – heat capacity of air at constant volume. With increasing temperature, the air density decreases, and the value c_v increases. Therefore an evaluation of plasma cord temperature according to Equation (1) is approximate.

If breakdown voltage is U = 6 kV, C = 3.3 nF, the discharge energy $W_0 = \frac{CU^2}{2} =$ 5.9 10^{-2} J. For discharge gap length ℓ = 3 mm and diameter of plasma cord ~ 0.7 mm (the cord diameter was visually estimated by photographing the spark), the temperature of the heated plasma cord according to Equation (1) is ~ 1.3 x 10^4 K. In the case of black body radiation according to Wien's displacement law, the maximum emission spectrum (λ_{max}) is connected to a body temperature (T): λ_{max} = 2.9 x 10^{-3}/T (K). At T~1.3 x 10^4 K, λ_{max}=220 nm. This radiation will pass through the air and enter the liquid, so the choice of capacitance C = 3.3 nF is justified. The temperature T~1.3 x 10^4 K corresponds to the average kinetic energy of gas molecules at about 1.5 eV (E = (3/2)kT, k – Boltzmann constant). The ionisation potentials of the main air components are: oxygen 13.6 eV, nitrogen 14.5 eV. Therefore the degree of gas ionisation in discharge region is small, and the production of active species (radicals) in the discharge region is negligible. The conclusion that plasma degree ionisation for discharge, used in our work, is small, is confirmed by the absence of oxidising agents in the gas (this will be elaborated upon later), and by the nature of the dependence of the chemical effect of the power pulse electric discharge.

Increasing capacitance C at the constant breakdown voltage of the spark gap leads to an increase in the plasma cord temperature and the spectral maximum of radiation being displaced in the vacuum ultraviolet region with λ < 200 nm. The radiation with λ < 200 nm is strongly absorbed in air, and it does not reach the surface of the object to be processed. Because of the loss of radiation with λ < 200 nm, the efficiency of the UVC radiation source decreases. The decrease of the chemical effect with increasing discharge capacity C confirms that the position of maximum UVC radiation is at a wavelength longer than 200 nm.

Chemicals produced under low ionised plasma radiation of spark electric discharge in gas phase

Active species, generated in discharge itself during the leading edge of the current pulse, must first of all terminate in interactions between themselves, as in the discharge region there are no other chemicals to interact with whom they could be spent [7]. As a result of active species interactions in the discharge region, non-active products can be formed, which will diffuse from the place of formation on the vessel walls and the surface of the treated water. Due to the fact that, in this case, there is no directional flow of gas from the discharge area towards a treated object, a direct hit of the active species from the discharge region is excluded.

The first analysis is made in the content of gas phase ozone. For this purpose, the gas was withdrawn from the reaction vessel within 30 minutes, when radiation source was turned on, and fed into the chemiluminescent ozone analyzer. Ozone has not been detected, and the sensitivity of the device is 10^{-6} g O_3/m^3. Hence, the ozone concentration in the gas phase is $[O_3] < 2 \times 10^{-8}$ mol/m^3.

To assess the content of oxidising agents in the gas phase when discharge is turned on, the gas is aspirated from the reaction vessel and blown through 5% KI solution with velocity 0.5 l/min. After blowing for 30 minutes, a colour appearance of KI solution was not observed. By titration with sodium thiosulphate (0.02 N) in an acidic medium, we determine the limit I_2 concentration, which can be detected. Hence the oxidant concentration in the gas phase is $[ox] < 2 \times 10^{-5}$ mol/l.

Thus, the entrainment of active species from the discharge region was not observed, since they almost all terminated in interactions with each other, and no gas was blown through the discharge region. The probability of active species creation in the gas phase itself under plasma radiation is small, since the gas density is much less than the liquid density, and the absorption of radiation energy in gas does not exceed 0.1% of full radiation energy.

Non-active chemicals formed in the discharge region and diffusing on the vessel wall and the treated object were investigated by IR absorption spectra. These chemicals were absorbed by potassium bromide, KBr, transparent in the infrared range. Powder KBr weighing 0.5 g was poured on a Petri dish instead of water (see Fig. 1a). Measurements were carried out for two conditions: 1) in the absence of water in dry air; 2) in the presence of water vapour, on the bottom of reaction vessel was poured 5 ml water. After treatment for 30 minutes, KBr powder was compressed into tablets and IR spectra were measured by IR-Fourier spectrometer FSM 1202 (Russia, St. Petersburg). When the discharge treatment was made in dry air, no lines in the IR-spectra were observed. The spectrum measured in wet air (on the bottom of vessel was water) for the range of wavenumbers ν from 2000–700 1/cm is shown in Fig. 4. The main absorption line is at ν ~ 1380–1370 1/cm. A more detailed analysis of IR spectra is given in [8]. The observed absorption line can be attributed to group N=C-O [9]. Products containing such groups could be formed at the discharge of moist air into the environment of water vapour, carbon dioxide, oxygen and nitrogen. After formation in the discharge region, these products diffuse throughout the volume of reaction vessel and fall to the surface of the KBr powder.

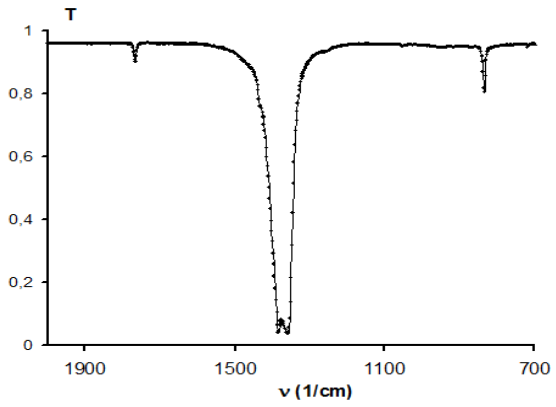

Figure 4. IR absorption spectrum of KBr crystal after treatment in reaction vessel with water vapour during 30 minutes. T – transmittance, ν - wavenumber, 1/cm.

Species, produced in water

Change of water sample pH after treatment with radiation of low ionised plasma

The main effects in a water sample after treatment with radiation of low ionised plasma of spark discharge are a decrease in pH and an accumulation of oxidants and reductants [6]. Reduced pH in the processing is associated with the accumulation of NO_2^- and NO_3^- ions. After treatment of the samples for 14 days, the reduction of pH was continued. There was an appearance in the composition of products in 3–14 days after treatment of peroxinitrite and peroxinitrous acid [10]. The reason for this may be the formation during irradiation of the long-lived complex decaying within 14 days into peroxinitrite and peroxinitrous acid. In view of the short lifetime of peroxinitrite and peroxinitrous acid (~ 1 s) [11] their direct observation in the conditions of the experiment is impossible.

For the identification of the resulting products, the absorption spectra of the treated water in the range of 200–400 nm were measured [10]. The absorption line for NO_2^- ions is at wavelength 360 nm, extinction coefficient ε = 18 l(mol cm)$^{-1}$, for NO_3^- ions at λ = 301 nm, ε = 7 l(mol cm)$^{-1}$ [10]. The 301 nm line can contribute peroxinitrite ε = 1670 l(mol cm)$^{-1}$ [11]. Immediately after treatment for 20 minutes, the acidity is pH = 3.1. In the spectrum of absorption immediately after treatment, only the line of nitrous acid (360 nm) was found. By means of ion-selective electrodes, the concentrations of ions NO_2^- and NO_3^- were measured. The values of the concentrations are $[NO_2^-]$ = 0.005 $\pm$ 0.0015 mol/l and $[NO_3^-]$ = 0.0008 $\pm$ 0.00015 mol/l. In view of small concentrations of NO_3^- ions, nitric acid in the absorption spectra was not found.

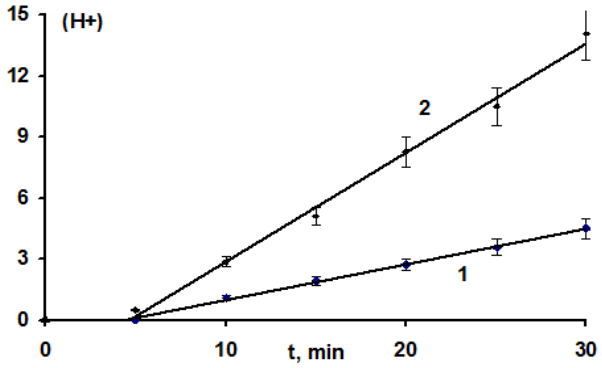

Figure 5. Initial part of time dependence content of ions (H^+) = $[H^+]$xVx10^5 (mol) in water samples, treated with spark discharge low ionised plasma radiation. Time treatment: t – minutes, water sample volumes: 1 – V = 45 ml, 2 – V = 300 ml.

The time dependence of hydrogen ions content in the sample, calculated from pH value as: (H^+) = $V[H^+] = Vx10^{-pH}$, where V – volume of sample. Results for two different samples of water V = 45 ml and 300 ml for time treatment with plasma radiation for up to 30 minutes are shown in Fig. 5. The treatment was made in vessel (600 ml in volume; bottom diameter of 90 mm). The distance from the water surface to the radiation source in both cases was the same: 60 mm. In the first case (curve 1, Fig. 5) on the vessel bottom was placed a Teflon Petri dish of 60 mm inner diameter, while the water layer thickness was 13 mm. In the second case (curve 2, Fig. 5) 300 ml of water was poured into a vessel, and the water layer thickness was 47 mm. It is seen from Fig. 5 that in both cases, the dependence (H^+) on time treatment is linear. A notable increase in H^+ ions content, related to acid production, starts ~ 5 minutes after the start of treatment. This is due to the establishment of the steady state concentration of products in water. Acids were formed from the intermediates that were not present at the beginning of treatment. The concentration of hydrogen ions increases with the formation of acidic residue ions. By means of ion selective electrodes in the solution, we identified ions NO_2^- and NO_3^-. Their concentration increases, and when the steady-state concentration of intermediate products is achieved, the linear increase of hydrogen ions in solution starts. The content of hydrogen ions in the sample of volume 300 ml is essentially greater than in the 45 ml sample. This means that the secondary species was generated by the action of low ionised plasma radiation in the water itself. When radiation passes through water, it is absorbed by the upper layers of the liquid; part of the beam energy is

ISSN: 0975-8585

consumed, and therefore the photon flux decreases with the thickness of the liquid layer. The yield of hydrogen ions increases with increasing layer thickness, but not in proportion with the volume of water due to the absorption of radiation.

The time dependence of pH (curve 1) and concentration of hydrogen ions [H^+] (curve 2) in the sample volume of 45 ml during treatment with radiation low ionised spark discharge plasma, up to a time of 120 minutes, are shown in Fig. 6. The concentration of hydrogen ions increases linearly with time. During the first five minutes, the increasing rate is small, and is associated with the establishment of a steady-state concentration of active intermediate products. On the same Fig. 6 (curve 3) there is the time dependence of pH for the water sample of 45 ml, treated with UVC radiation from the mercury lamp. The pH value does not decrease: it has a slight tendency to increase, although the flux of UVC photons from the mercury lamp is 430 times greater than the pulse radiation flux of low ionised plasma (see Table 1).

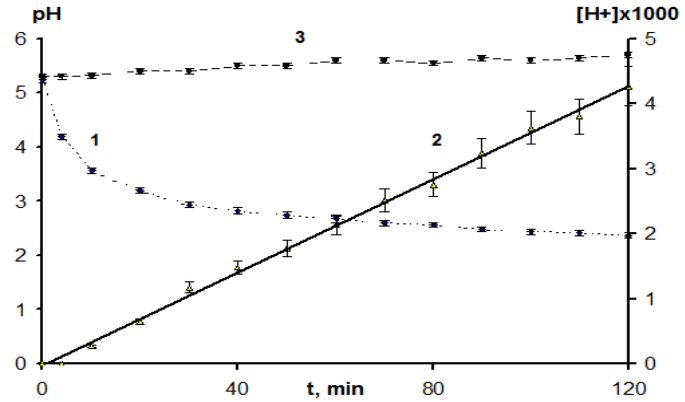

Figure 6. The dependence of pH (curve 1) and hydrogen ion concentration [H^+]x1000 mol/l (2) for sample of water (45 ml) from treatment time to pulse plasma radiation t, min; 3 – time dependence of pH of water sample (45 ml) during treatment with continuous radiation from the mercury lamp.

The analysis of water using Nessler's reagent showed that in the water there are NH_4^+ ions. After 10 minutes' treatment with plasma radiation in volume 4 ml, the concentration is [NH_4^+] ~ 100 μg/l. The velocity of NH_4^+ ion production is $(1.7 \pm 0.5) \times 10^{-10}$ mol/(l s). Under radiation of the mercury lamp, the rate of NH_4^+ ion formation is essentially greater, equal to $(2.5 \pm 1.5) \times 10^{-8}$ mol/(l s).

Evaluation of concentration of ozone and hydrogen peroxide in water

Estimation in the treated water of hydrogen peroxide was carried out by reacting the peroxide with a freshly prepared titanium trichloride ($TiCl_3$) [12]. The reagent was prepared immediately before the measurement by dissolving titanium metal in hydrochloric acid. The complex formed in reaction with hydrogen peroxide has an absorption line in the yellow-orange region of the spectrum λ = 410 nm. Hydrogen peroxide within the measurements error is not detected, $[H_2O_2] < 5 \times 10^{-5}$ mol/l. The evaluation of ozone concentration in water was carried out by measuring the absorption spectrum immediately after treatment with plasma radiation during 20 minutes at wavelength 260 nm. The extinction coefficient for ozone was ε = 3290 $(\text{mol cm})^{-1}$ [13]. In the limit of measurement errors, ozone in the treated water was not found, i.e. $[O_3] < 10^{-5}$ mol/l.

Yield evaluation of hydroxyl radicals in water under low ionised plasma radiation

It was shown in [6, 10], that the main primary active species, which can produce radicals $HO_2^\bullet$, $O^\bullet$ and molecules N_2O under pulsed UVC radiation in the scope of the energy conservation law at wavelengths $200 \leq \lambda \leq 280$ nm. In further transformations of the primary species, a secondary species can form, which can be a radical $OH^\bullet$. However, its yield is very small, quickly spent in interactions with each other and with other secondary active species.

For direct experimental yield of radicals $OH^\bullet$ and $HO_2^\bullet$ oxalic acid and Mohr's salt were used. Oxalic acid can be oxidised only by $OH^\bullet$ radicals [14] and cannot be oxidised by $HO_2^\bullet$ radicals. $HO_2^\bullet$ radicals oxidise Mohr's salt. Aqueous 0.02 N solution of oxalic acid and 0.01 N solution of Mohr's salt in sulphuric acid (pH = 2)

45 ml volume were treated with plasma radiation for 30 minutes. The concentrations of oxalic acid and bivalent iron in Mohr's salt were determined by titration with 0.05 N potassium permanganate in an acid medium at a temperature of 80 °C. Changing concentrations of oxalic acid under low ionised plasma radiation was not detected. Hence the concentration of $OH^{\bullet}$ radicals did not exceed 10^{-8} mol/l. The rate of $HO_2^{\bullet}$ radical production (i.e. the rate of oxidation bivalent iron in Mohr's salt) is $(1.2 \pm 0.3) \times 10^{-6}$ mol(l s)$^{-1}$.

The same experiments were made with radiation from the mercury lamp. It was found that the yield of $HO_2^{\bullet}$ radicals is $(1.1 \pm 0.5) \times 10^{-6}$ mol(l s)$^{-1}$. The yields of $HO_2^{\bullet}$ radicals under pulse plasma radiation and continuous radiation from the mercury lamp are the same, although the flux of mercury lamp photons is 430 times greater than the radiation of spark discharge.

The second stage dissociation constant for 0.01 N oxalic acid solution was determined by titration with 0.1 N NaOH:

$$HOOC\text{-}COO^- \leftrightarrow {}^-OOC\text{-}COO^- + H^+ \qquad (2)$$

The titration results for initial solution and solution after treatment with plasma radiation for 30 minutes are shown in Fig. 7. In the same figure, for comparison, the titration curve of nitric acid (pH = 2.77) is shown. The oxalic acid after plasma radiation treatment for 30 minutes keeps its buffering properties. The value of the constant of second stage dissociation was determined. The results are: for the initial solution $pK_{a2} = 4.25 \pm 0.15$, and for the treated solution $pK_{a2} = 4.3 \pm 0.2$. The constant dissociation did not change in the limit of experimental errors and agrees with the known value [18] $pK_{a2} = 4.14$.

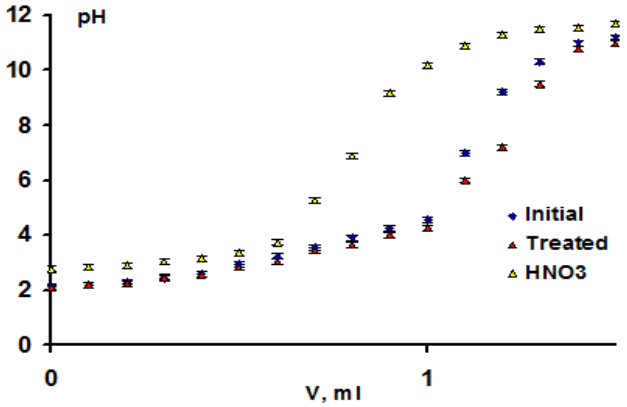

Figure 7. Titration with 0.1 N NaOH of the sample of non-treated oxalic acid (Initial) and sample after treatment with plasma radiation for 30 minutes (Treated). Oxalic acid concentration was 0.01 N. For comparison: titration of nitric acid sample with pH = 2.77 (HNO_3).

Changes in composition of products after treatment with pulse radiation of low ionised plasma

The main stable products, appearing under pulse radiation of low ionised plasma, are ions of nitrous and nitric acids NO_2^- and NO_3^-. Nitrous acid is weak, with dissociation constant $pK_a = 3.4$. At $pH < pK_a$ a significant portion of nitrous acid remains undissociated and does not contribute to the value $[H^+]$, measured by pH electrodes. Therefore a chemical method was used to evaluate the acidity of the water. Water, treated with plasma radiation for 20 minutes, was titrated with alkali: 0.025 N NaOH. By means of titration, the presence of a weak acid in the water was found. The measurement with electrodes gave the value pH = 3.1, but titration with alkali gave the concentration of H^+ ions, which corresponded to pH = 2.7. During the titration it was considered that titration product is $NaNO_2$, giving an alkaline reaction, whereby the neutralisation point does not coincide with the equivalence point. The weak acid not completely dissociated, so measurement with electrodes gave the concentration of hydrogen ions in solution, and does not take into account the hydrogen ions in the bound state. Results for titration of water samples immediately after treatment and during 14 days after are shown in Fig. 8. The total concentration of acid anions in samples does not change and corresponds to the value pH = 2.7. Weak acids non-dissociated in acid media can be nitrous acid ($pK_a = 3.4$) and peroxinitrous acid ($pK_a = 6.8$). Peroxinitrous acid can arise after long-living complex decay. From Fig. 8 it is

ISSN: 0975-8585

seen that after 14 days, both acids are decayed, and the values of pH, determined by titration with alkali and with electrodes, are the same.

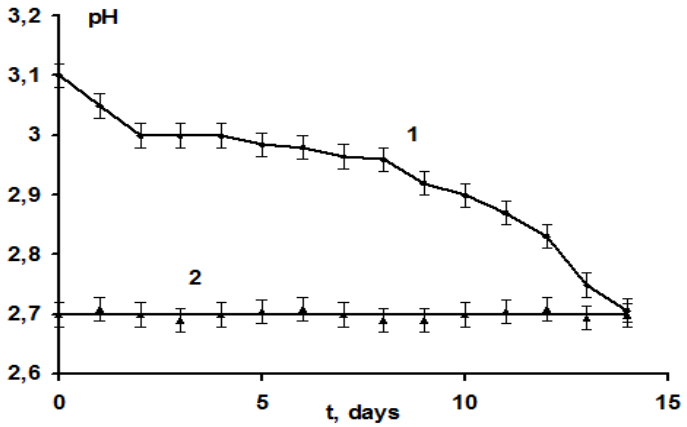

Figure 8. Dependence of pH value for water sample of 45 ml, treated with pulse radiation of low ionised spark air-discharge plasma for 20 minutes, determined by electrodes (1) and alkali NaOH titration (2) from time after treatment t, given in days. pH value at t = 0 was measured immediately after treatment.

In the composition of products generated by radiation, we identified nitrous, nitric acids and complex, decayed on peroxynitrite and peroxynitrous acid during 14 days after treatment [10]. To compare the decay of pure nitrous acid with decay of species produced under radiation, a following experiment was performed. Water samples 45 ml in volume treated with plasma radiation for 30 minutes were prepared. The amount of 0.02 N sodium thiosulphate consumed for the titration of the water sample after the introduction of 5 ml sulphuric acid (1:4) and 5 ml 5% KI was determined.

Oxidation I^- could occur with nitrous acid and with peroxynitrite/peroxynitrous acid, formed by the decay of the complex. Water samples, each 45 ml in volume, and with treatment time of 30 minutes, were placed in separate containers and were accumulated. These samples were kept for a period of 1–14 days, and then the presence in the sample of active species was determined iodometrically. The measurements were performed for 4–5 samples. The results of water samples titration, immediately after treatment and kept for a period of 1–14 days, are shown in Fig. 9, curve 1. To evaluate the oxidation of I^- only by nitrous acid, the 0.005 mol/l $NaNO_2$ aqueous solution was prepared (equal to NO_2^- concentration in the water sample immediately after treatment). In the $NaNO_2$ solution, we added the concentrated nitric acid, and the pH value was made 2.8, as in the water samples after radiation treatment. For experimental evaluation of I^- oxidation possibility by nitric acid, the titration reactive (5 ml sulphuric acid (1:4) and 5 ml 5% KI) was added in the nitric acid water solution with pH = 2.5–2.8. No changes of colour solution during the 5 minutes were observed, so the nitric acid did not oxidises I^-. Nitrous acid oxidises the I^- according to the following reaction:

$$2I^- + 4H^+ + 2NO_2^- \rightarrow I_2\downarrow + 2NO^{\bullet}\uparrow + 2H_2O \qquad (3)$$

Nitrous acid (pK_a = 3.4) at pH = 2.8 is weakly dissociated, but Equation (3) completes, when the NO_2^- ions consumed the remaining HNO_2 molecules dissociate. This is a slow process, so before the titration a sample was incubated for 5 minutes. In the acid solution $ONOOH/ONOO^-$ exists predominantly in the form of peroxinitrous acid, $pK_a(ONOOH/ONOO^-)$ = 6.8 [11]. Peroxinitrous acid also oxidises I^-:

$$2ONOOH + 2I^- \rightarrow I_2\downarrow + 2NO^{\bullet}\uparrow + H_2O \qquad (4)$$

The titration results for solution $NaNO_2$ + HNO_3 immediately after preparing and during 14 days of storage are shown in Figure 9, curve 2. In acid media, NO_2^- ions slowly decompose with the release of $NO^{\bullet}$ and formation of nitric acid. Therefore, over time, consumption of 0.02 N thiosulphate for titration $NaNO_2$ + HNO_3 solution decreases from 14 ml immediately after preparation to 0.1 ml after 14 days.

ISSN: 0975-8585

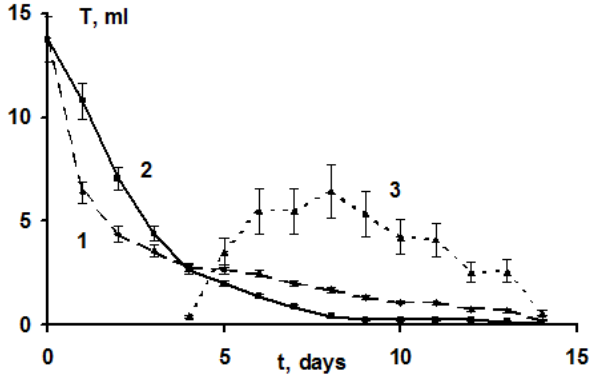

Figure 9. Consumption of 0.02 N sodium thiosulphate (T, ml) for titration of the sample 45 ml in volume through t days after preparation: 1 – water, treated with plasma radiation for 30 minutes; 2 – solution $NaNO_2$ + HNO_3, pH = 2.8; 3 – the difference (T1 – T2) x 5.

If in the water sample under plasma radiation the complex is formed, which decays to ONOOH/$ONOO^-$, the complex decay products in acid media will interact with NO_2^- ions [15]:

$$ONOOH + NO_2^- \leftrightarrow adduct^- \rightarrow NO_2^- + NO_3^- + H^+ \qquad (5)$$

The rate of Equation (5) is strongly dependent on the reagent concentration. The concentration of the NO_2^- ions decreases in Equation (5). The observed rate constant for Equation (5) is k_{5obs} = 1.1–6 c^{-1} [15]. Peroxynitrous acid and NO_2^- ions are spent.

The consumption of thiosulphate for titration of $NaNO_2$ + HNO_3 solution decreases with a keeping time only due to the expenditure of NO_2^- ions. In the water sample, treated with plasma radiation, for the same initial concentration of NO_2^- ions the decreasing of thiosulphate consumption for titration causes the decomposition of NO_2^- ions in acid media and the consumption of NO_2^- ions in Equation (5). Therefore, in the sample of treated water during first three days, the consumption of thiosulphate for titration decreases faster than in the solution $NaNO_2$ + HNO_3. When the concentration of NO_2^- ions on fourth day after treatment is decreased, the consumption of peroxinitrous acid in Equation (5) also decreased. The role of Equation (4) in oxidation of I^- is increased, and the contribution of peroxinitrous acid in the production of I_2 becomes predominant. During first three days, almost all the peroxinitrous acid is consumed in Equation (5); therefore peroxinitrite and peroxinitrous acid in [10] during the first three days were not determined. They are noticeable on the third and fourth days after treatment. Their yield reaches a maximum during the seventh to ninth days after treatment, when NO_2^- ions almost completely disintegrate. Titres difference T1 – T2 (curve 3) becomes larger than zero on the fourth day and reaches its maximum during the seventh to ninth days.

Thus, for the first three days after treatment, peroxinitrite and peroxinitrous acid are consumed in Equation (5) with NO_2^- ions. The peroxinitrite and peroxinitrous acid become visible after the NO_2^- ions decay and completely disappear on the 14th day, when the complex is decayed. The concentration of the complex, which can be obtained on the basis of the results of the titration, is (2.5 $\pm$ 0.5) x 10^{-3} mol/l. This value agrees with the results obtained in [10]: (1.8 $\pm$ 0.4) x 10^{-3} mol/l. Table 1 shows the final results of the determination of the active species yields and their concentrations in water under the action of the used UVC radiation sources.

DISCUSSION

Mechanism of primary active species generation in water under pulse air discharge low ionised plasma radiation

As shown by the experimental evaluation, plasma, produced in spark discharge with parameters, selected in this work, is low ionised. Active species in discharge region can appear only in time of the leading edge of the discharge pulse, when electric field strength in the discharge gap is large. However, this stage is

very short; it takes less than 0.1% of full pulse duration time. The active species is terminated in second stage, when in the discharge gap the main energy of discharge is allocated, and the discharge becomes an arc. As a result in the discharge itself are produced only stable non-reactive products. The temperature of the spark cord is not sufficient to ionise gas molecules; therefore active species in the time of the main phase, when discharge becomes an arc, are not produced.

Chemical activity has radiation of low ionised plasma. Passing through the air, radiation produces a negligible chemical effect, since the density of air is much less than the density of water and the energy, absorbed by air, does not exceed 0.1% of the total energy of the beam. Therefore, the main chemical effect is produced by radiation in the treated liquid. Processes leading to the generation of chemically active species in water under pulse radiation of air spark discharge low ionised plasma, are illustrated in Fig. 10.

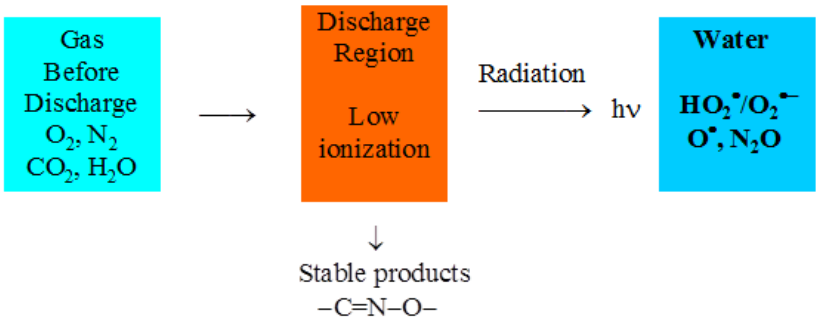

Figure 10. Stages of formation of chemically active species under radiation low ionised plasma of air spark discharge.

We now consider the power relations that determine the possibility of species formation under light radiation. The energy of UVC radiation with wavelength 200–280 nm varies from 6.2 eV (597 kJ/mol) to 4.43 eV (427 kJ/mol). First we evaluate the possibility of hydroxyl radical creation. A possible mechanism of hydroxyl radical creation in water could be the process:

$$H_2O + h\nu \rightarrow OH^{\bullet} + H^{\bullet} \quad (6)$$

The bond dissociation energy of the water molecule is 485 kJ/mol [16]. This photon has an energy of 5.03 eV (485 kJ/mol), when $\lambda \sim 246$ nm. This means that under UVC radiation with $\lambda < 246$ nm, the break-up of water molecules with the production of hydroxyl radicals is possible. However, the probability of this process is very small [17]. Hydroxyl radicals can be produced with appreciable probability at $\lambda < 180$ nm. Therefore, the probability of direct hydroxyl radical production in water under UVC radiation is negligible.

The excited molecule of water can be formed under UVC radiation. The local density of excited molecules in short-time radiation pulses is high; therefore they can interact with each other. The sum energy of two excited water molecules is sufficient to produce radicals $HO_2^{\bullet}$ after their interaction:

$$H_2O + h\nu \rightarrow H_2O^* \quad (7)$$
$$H_2O^* + H_2O^* \rightarrow HO_2^{\bullet} + H_2 + H^{\bullet} \quad (8)$$
$$H^{\bullet} + H^{\bullet} + H_2O \rightarrow H_2 + H_2O \quad (9)$$

For radicals $HO_2^{\bullet}/O_2^{\bullet-}$ there is an equilibrium [11]:

$$HO_2^{\bullet} \leftrightarrow O_2^{\bullet-} + H^+, \; pK_a = 4.8 \quad (10)$$

Since the acidity of the water under radiation low ionised plasma rapidly decreases up to pH < 4.8, the radical $HO_2^{\bullet}/O_2^{\bullet-}$ under the conditions of this experiment exists predominantly in the form $HO_2^{\bullet}$.

There are dissolved gases in water: nitrogen and oxygen. Molecules of nitrogen and oxygen can go into excited states under pulses of UVC radiation. The energy of UVC photons with $\lambda < 250$ nm is sufficient to realise the following process:

$$N_2 + O_2 + h\nu \rightarrow N_2^* + O_2^* \rightarrow N_2O + O^\bullet \quad (11)$$

It should be emphasised that Equation (11) is possible only by interaction of two excited molecules: nitrogen and oxygen. The probability interaction of two excited molecules is increased with their concentrations. The maximum instantaneous concentration of excited molecules is achieved under pulsed radiation. The probability of this process with a beam of continuous UVC radiation is small, as a local concentration of excited molecules N_2^* and O_2^* is small. In fact, we do not observe the pH decreasing under continuous radiation of the low-pressure mercury lamp, although the flux of photons in the UVC range of the mercury lamp is 430 times greater than the mean photon flux from low ionised plasma radiation.

The dissociation energy of oxygen molecule O=O is 494 kJ/mol [16]. Therefore under UVC radiation with $\lambda < 242$ nm, the dissociation of the oxygen molecule dissolved in water is possible.

$$O_2 + h\nu \rightarrow 2O^\bullet \quad (12)$$

Production of secondary active species

Interaction of primary active species leads to the production of secondary species. Let us evaluate a possible composition of secondary species and its interaction. First of all, ozone production is possible:

$$O_2 + O^\bullet + M \rightarrow O_3 \quad (13)$$

The interaction of $HO_2^\bullet$ radicals and ozone leads to the formation and consumption of hydroxyl radicals [18]:

$$HO_2^\bullet + O_3 \rightarrow OH^\bullet + 2O_2 \qquad k = 1.2\ 10^6 \quad (14)$$
$$OH^\bullet + O_3 \rightarrow HO_2^\bullet + O_2 \qquad k = 4\ 10^7 \quad (15)$$

In these reactions, ozone is consumed, produced and consumed the hydroxyl radical. The rate of consumption of the hydroxyl radicals in Equation (15) exceeds the rate of their production in Equation (14); therefore the hydroxyl radicals do not accumulate. Hydrogen peroxide can be produced at the interaction of $HO_2^\bullet$ radicals [18]:

$$HO_2^\bullet + HO_2^\bullet \rightarrow H_2O_2 + O_2 \qquad k = 8.3\ 10^5 \quad (16)$$

The resulting hydrogen peroxide is consumed in the reaction with hydroxyl radicals [18]:

$$H_2O_2 + OH^\bullet \rightarrow HO_2^\bullet + H_2O \qquad k = 3\ 10^7 \quad (17)$$

The rate constant of consumption of hydrogen peroxide (Equation 17) exceeds the rate of its production (Equation 16). As a result of the reactions (14–17) the ozone, hydrogen peroxide and hydroxyl radicals are produced, but are spent in interactions with each other. The final product of these interactions is radical $HO_2^\bullet$, which initiates Equations (14) and (16).

Therefore the dissolved ozone, hydroxyl radicals and hydrogen peroxide in water after treatment with radiation of low ionised plasma air spark electric discharge are not found. Simulation of these processes in [19] shows that the concentration of O_3, H_2O_2 and $OH^\bullet$, produced under pulse plasma radiation for air spark discharge is small, as they terminate in interactions with each other.

In this case, when continuous UVC radiation acts on water, the situation changes. The instantaneous concentration of excited water molecules is small, and the probability of its interactions strongly decreases. Therefore in our work under UVC radiation of the mercury lamp, only radicals $HO_2^\bullet$ were found, but a decrease of pH was not observed (see Fig. 6). The yield of radicals $HO_2^\bullet$ was the same as that under the action of pulsed radiation, although the average intensity of mercury lamp radiation was 430 times greater than for pulse radiation of spark discharge.

Consider the chain of further chemical conversions of primary active species, which can lead to acid production (i.e. decreasing pH). Among the secondary active species, the more interesting ones are nitric oxide $NO^{\bullet}$, nitrous and peroxinitrous acids, and peroxinitrite. The mechanism of nitric oxide production can be the following reaction:

$$N_2O + O^{\bullet} \rightarrow 2NO^{\bullet} \quad [18] \quad k=4.3 \times 10^{10} (mol\ s)^{-1} \quad (18)$$

The production of nitrous acid can be by the following reactions:

$$NO^{\bullet} + O^{\bullet} + M \rightarrow NO_2^{\bullet} + M \quad [18] \quad k=1.8 \times 10^{10} (mol\ s)^{-1} \quad (19)$$

$$NO^{\bullet} + NO_2^{\bullet} + M \rightarrow N_2O_3 + M \quad [20] \quad 8 \times 10^{7} (mol\ s)^{-1} \quad (20)$$

$$N_2O_3 + H_2O \rightarrow 2HNO_2 \quad [21] \quad k = 18 (mol\ s)^{-1} \quad (21)$$

$$3HNO_2 \rightarrow HNO_3 + 2NO^{\bullet} + H_2O \quad [21] \quad k= 10^{-3} (mol\ s)^{-1} \quad (22)$$

$$NO_2^{\bullet} + NO_2^{\bullet} + M \rightarrow N_2O_4 + M \quad [20] \quad k=5 \times 10^{10} (mol\ s)^{-1} \quad (23)$$

$$N_2O_4 + H_2O \rightarrow HNO_3 + HNO_2 \quad [21] \quad k = 10.8 (mol\ s)^{-1} \quad (24)$$

Based on the magnitude of the rate constants of the reactions above, we can say that in these reactions, nitrous acid most probably is produced. The probability of nitric acid production is less.

Furthermore, the formation of peroxinitrite and peroxinitrous acid is possible. The main mechanisms of peroxinitrite and peroxinitrous acid production in the case of our experiment are the following reactions [22, 23]:

In neutral and alkali solutions:

$$O_2^{\bullet -} + NO^{\bullet} + M \rightarrow ONOO^{-} + M \quad k = 3.8\ 10^{9} (mol\ s)^{-1} \quad (25)$$

In acidic solutions:

$$HO_2^{\bullet} + NO^{\bullet} + M \rightarrow ONOOH + M \quad k = 3.2\ 10^{9} (mol\ s)^{-1} \quad (26)$$

Isomerisation of peroxinitrous acid leads to the production of nitric acid [24]:

$$ONOOH \rightarrow HNO_3 \quad (27)$$

The probability of direct nitric acid production (Equation 24) compared to peroxinitrous acid production (Equation 26) is essentially less: see the values of the reaction constants. Therefore, the main path of nitric acid production is through formation and decay of peroxinitrous acid (Equations 26, 27).

An additional mechanism for peroxinitrous acid production could be the reaction [25]:

$$H_2O_2 + NO_2^{-} + H^{+} \rightarrow ONOOH + H_2O \quad k = 1.1\ 10^{3} (mol\ s)^{-1} \quad (28)$$

Immediately after treatment, the concentration of NO_2^{-} is about 5×10^{-3} M and $[H_2O_2] < 10^{-4}$ M. The rate of peroxinitrous acid production for a given pulse duration and pulse repetition frequency could be about 10^{-9} $(mol\ s)^{-1}$. However, in fact, we do not see the hydrogen peroxide, and this production rate is an upper limit. With the rate 10^{-9} $(mol\ s)^{-1}$ in the course of treatment over 1800 s (taking into account the pulse duration), about 10^{-6} M of peroxynitrous acid could be produced. This yield is very small compared to the experimental value (10^{-3} M), obtained in our work and in [10]. Therefore we can state that Equation (28) does not play an essential role.

ISSN: 0975-8585

Chemical activity of main species

Radicals $HO_2^{\bullet}$

Now we estimate the chemical activity of $HO_2^{\bullet}$ radicals for an example reaction with oxalic acid, and compare it to the reactivity of hydroxyl radicals. For these radicals we give a typical abstraction reaction of the hydrogen atom. In this reaction, energy is released equal to the binding energy of the resulting molecule [16].

$$OH^{\bullet} + H^{\bullet} \rightarrow H_2O \qquad E = 481 \text{ kJ/mol} \qquad (29)$$
$$HO_2^{\bullet} + H^{\bullet} \rightarrow H_2O_2 \qquad E = 368 \text{ kJ/mol} \qquad (30)$$

The energy released in Equations (29) and (30) is spent on abstraction of a hydrogen atom from oxidised molecules. If this energy is more than the energy of hydrogen bond in molecule that reacts with the radical, the abstraction of hydrogen atom is possible.

The bond energy of –COO–H in oxalic acid molecule is ~ 439 kJ/mol [16, 18]. The energy released in Equation (30) is insufficient to abstract (take away) hydrogen atom from oxalic acid. The oxalic acid can be oxidised with $OH^{\bullet}$ radicals and cannot be oxidised with $HO_2^{\bullet}$ radicals. Therefore, the oxalic acid was used in our work to evaluate the presence of hydroxyl radicals. Direct measurement of constant pK_{a2} second dissociation stage of oxalic acid made here (see Fig. 7) showed that the degradation of oxalic acid with $HO_2^{\bullet}$ radicals does not take place.

The energy of dissociation of the C-H bond for hydrocarbons is in the limits of 251–460 kJ/mol [16]. In saturated fatty acids, energy dissociation of the C-H bond is 381 kJ/mol. For unsaturated fatty acids, the separation energy of the hydrogen atom located in the α-position relative to the double bond is 364 kJ/mol. Thus the hydroxyl radical, which in Equation (29) releases energy 481 kJ/mol, can oxidise any organic compound (i.e. any saturated and non-saturated fatty acid). The radical $HO_2^{\bullet}$ can oxidise only non-saturated fatty acids that have at least one double bond.

Peroxinitrite and peroxinitrous acid

When considering the chemical properties of peroxinitrite, IUPAC oxoperoxonitrate(1–) and peroxinitrous acid (IUPAC hydrogen oxoperoxonitrate) first of all their oxidising ability is taken into account [24]. The oxidising ability manifests in the decay through the channels to form in the final state of nitrous acid. Peroxinitrous acid (peroxinitrite) is a strong one electron and two-electron oxidant. Peroxinitrous acid is the main form of $ONOOH/ONOO^-$ (pK_a = 6.8) in acidic solution. An acidic solution is quickly achieved in water under spark discharge plasma radiation. The oxidative properties of peroxinitrous acid are realised in the case of decay through the channels [26]:

$$ONOOH + H^+ + e^- \rightarrow NO_2^{\bullet} + H_2O \quad (E'^{\circ}pH{:}7 = 1.6 \text{ V}) \qquad (31)$$
$$ONOOH + 2H^+ + 2e^- \rightarrow HNO_2 + H_2O \quad (E'^{\circ}pH{:}7 = 1.3 \text{ V}) \qquad (32)$$

In these processes, the oxidative power of nitrogen does not change: nitrogen remains trivalent (oxidation power 3+): see 32a.

(32a)

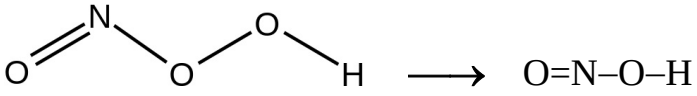

Isomerisation of peroxinitrous acid leads to the production of nitric acid: see 33, 33a:

$$ONOOH \rightarrow HNO_3 \qquad (33)$$

ISSN: 0975-8585

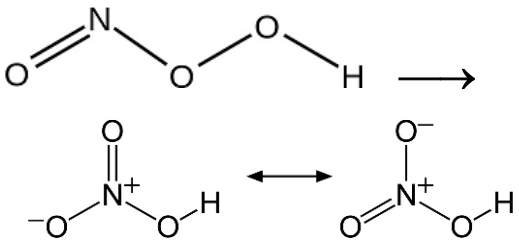

(33a)

Nitric acid is a strong acid, completely dissociated in water as $HNO_3 \rightarrow H^+ + NO_3^-$. In the course of isomerisation of peroxinitrous acid, the nitrogen atom oxidises by electron transfer from state 3+ to state 5+ (see 33a). Nitrites (state 3+) that are produced in 31 and 32, can be oxidants or reductants; in an acidic solution they are oxidised to nitrate (state 5+), while in an alkali solution, nitrite is reduced to nitric oxide $NO^{\bullet}$ (2+). In the course of nitrogen oxidation 3+ → 5+ (Equation 33), two-electron transfer occurs. These electrons will cause the reduction processes. Therefore, peroxinitrous acid can be both oxidant and reductant. Equation (33) is a net process [23, 25], one stage of which can be $H^{\bullet}$ radical production. The reduction of free stable radical $DPPH^{\bullet}$ in the course of treatment to low ionised plasma radiation was observed in [10].

Formation of complex long-lived, decaying to peroxinitrite and peroxinitrous acid

The chemical activity of the water treated to radiation of low ionised plasma of air spark electric discharge, was observed experimentally by a decrease of pH and a reduction of $DPPH^{\bullet}$ in [10]. The reduction can be attributed to peroxinitrous acid. The line 300 nm in UV spectra was observed after treatment of weakly acidic, neutral and alkaline water solutions, which can be attributed to peroxinitrite taking into account the contribution to this line of nitric acid [27]. The total yield of peroxinitrite in alkaline solution during 14 days after treatment to pulse radiation was $(1.2 \pm 0.5) \times 10^{-2}$ mol/l [27], which is 10 times greater than for an acidic solution. Peroxinitric acid and peroxinitrite complex production can be the cause for the iodine oxidation of water treated with plasma radiation 14 days after treatment (see Fig. 9).

Peroxinitrite and peroxinitrous acid have short lifetimes [24], and cannot be observed in conditions of the given experiment, even immediately after irradiation. The manifestation of their chemical activity after treatment indicates that peroxinitrite and peroxinitrous acid form during processing of long-lived compounds (complexes), which slowly decay over 14 days. The possibility of the formation of this complex was supposed in [28]. In an acidic solution, $ONOOH/ONOO^-$ exists as ONOOH. The first 3–4 days of peroxinitrous acid cannot be detected due to the fact that it is consumed in the reaction with nitrous acid (Equation 5). When the nitrous acid concentration decreases due to its disintegration in an acidic environment, arising in the decay of the complex, peroxinitrous acid begins to show chemical activity itself.

The observed concentration of peroxinitrous acid, evaluated on the basis of its reductive properties, and peroxinitrite concentration evaluated on the basis of absorbance in the peak at 300 nm for the time from three up to 14 days after plasma radiation treatment are approximately the same: $[ONOO^-] \sim [ONOOH] \sim 10^{-5}$ mol/l [29].

Production of a long-living chemical compound, which decays to peroxinitrite and peroxinitrous acid, could be the cause of the strong sporicidal effect after treatment of micromycet spores with spark gas-discharge low ionised plasma radiation, which is observed in [30]. Micromycet spores are covered with an opaque peptidoglycan layer, through which UV radiation as well as short-lived species (radicals) cannot penetrate easily. The species that persist from ~1 s up to 14 days can enter into the spore, where they decay to peroxinitrite and peroxinitrous acid. They cause irreversible damage of DNA molecules [31]. As a result, the spores do not grow out and a 100% sporicidal effect is achieved. An evaluation of cytotoxic effect mechanisms of gas discharge low ionised plasma radiation was made in [32].

The source of gas-discharge low ionised plasma radiation used in our work creates active species on the surface of the treated object in an area of about 10 cm^2. Radiation produces appreciable chemical and

biological effects. Therefore this source of gas-discharge low ionised plasma radiation can be used in biomedical investigations and, in view of its simplicity, may find a broader range of applications.

CONCLUSIONS

- A gas discharge source of low ionised plasma radiation generates active species in a treated object, which were finally transformed into nitric acid through intermediate peroxinitrite and peroxinitrous acid formation.
- The energy transfer from the discharge region to the Petri dish is realised without matter transfer: only by light photons. The key condition for the chemical effect of plasma radiation is discharge power optimisation.
- The primary active species are $HO_2^{\bullet}$, $O^{\bullet}$ and N_2O.
- A secondary active species in the acid medium is peroxinitrous acid, which finally decays to nitrous and nitric acids. Its cumulative concentration is [ONOOH] ~ 10^{-3} mol/l.
- Under pulse low ionised plasma radiation of spark gas-discharge in air, a complex is produced that decays to peroxinitrite and peroxinitrous acid over 14 days.

REFERENCES

[1] Steiner U.E. (2014) Fundamentals of photophysics, photochemistry and photobiology. In: Abdel-Kader M (Ed) Photodynamic therapy from theory to application. Chapter 2. P. 25-58. Springer-Verlag, Berlin, Heidelberg.

[2] Rohatgi-Mukherjee KK (2013) Fundamentals of photochemistry. 386 p. Publisher New Age International. New Delhi.

[3] Pattison, D.I. and M.J. Davies, (2006) Actions of ultraviolet light on cellular structures. EXS 96:131 – 157.

[4] Dobrynin D, Fridman Gregory, Friedman Gary, Fridman A (2009) Physical and biological mechanisms of direct plasma interaction with living tissue. New Journal of Physics 11:115020 (26pp).

[5] Brisset J-L, Moussa D, Doubla A, Hnatiuc E, Hnatiuc B, Youbi GK, Herry J-M, Naitali M, Bellon-Fontaine M-N (2008) Chemical reactivity of discharges and temporal post-discharges in plasma treatment of aqueous media: examples of gliding discharge treated solutions. Ind Eng Chem Res 47:5761-5781.

[6] Piskarev IM, Ivanova IP, Trofimova SV, Aristova NA (2012) Formation of active species in spark discharge and their possible use. High Energy Chemistry 46(5):343-348.

[7] Piskarev IM (1998) Conditions of initiating reactions in liquids by gas phase active particles. Russian Journal of Physical Chemistry 72(11):1793-1799.

[8] Ivanova IP, Trofimova SV, Karpel Vel Leitner N, Aristova NA, Arkhipova EV, Burkhina OE, Sysoeva VA, Piskarev IM (2012) The analysis of active products of spark discharge plasma radiation determining biological effects in tissues. Sovremennye Technologii v Medicine 2:20-28.

[9] Vasil'ev AV, Grinenko EV, Shchukin AO, Fedulina TG (2007) Infrakrasnaya spevtroscopia organicheskikh I prirodnykh soedineniy (Infrared spectroscopy of organic and natural compounds), Saint Petersburg, GLTA, P. 30.

[10] Piskarev IM, Uschkhanov VA, Trofimova SV, Ivanova IP (2015) Peroxynitrite and peroxynitrous acid production of gas-discharge spark plasma radiation. Research Journal of Pharmaceutical, Biological and Chemical Science 6(3):260-276.

[11] Koppenol W.H. (1998) The basic chemistry of nitrogen monoxide and peroxynitrite, Free Radical Biol. Med. 25(4/5): 385-391.

[12] Brisset J-L, Hnatic E (2012) Peroxinitrite: A re-examination of the chemical properties of non-thermal discharges burning in air over aqueous solution. Plasma Chem. Plasma Process 32:655-674.

[13] Moussa D, Doubla A, Kamgang-Youbi G, Brisset J-L (2007) Postdischarge long life reactive intermediates involved in the plasma chemical degradation of an azoic dye. IEEE Trans. On Plasma Science 35(2):444 – 453.

[14] Garoma T, Gurol MD (2005) Modelling aqueous ozone/UV process using oxalic acid as probe chemical. Environ. Sci. Technol. 39: 7966-7969.

[15] Maurer P., Thomas C.F., Kissner R., Rjiegger H., Greter O., Rothlisher U., Koppenol W.H. Oxidation of nitrite by peroxynitrous acid. (2003) J. Phys. Chem. 107: 1763-1769.

[16] Energii razryva khimicheskikh svyazey. Potentialy ionizatsii I srodstvo k electronu (Chemical Bond Energies, Ionization Potentials and Electron Affinity), Kondrat'ev V.N., Ed. Moscow: Izd. AN SSSR, 1962.
[17] H. Okabe, Photochemistry of Small Molecules, New York, Wiley, 1978.
[18] CRC Handbook of Chemistry and Physics. 96TH Edition. Ed. W.M. Haynes. 2015-2016.
[19] Piskarev I.M., Ivanova I.P. and Trofimova S.V. (2013) Chemical effects of self-sustained spark discharge: simulation of processes in a liquid. High Energy Chem. 47(2): 62 – 66.
[20] M.G. Mc Ewan, L.F. Phillips. Chemistry of the Atmosphere. Edward Arnold. New York: Wiley.1975.
[21] Deminskii M.A., Ermakov A.N., Poskrebyshev G.A., Potapkin B.V., Rusanov V.D. (1999) High Energy Chem. 33(1): P. 40.
[22] W.H. Koppenol, J.J. Moreno, W.A. Pryor, H. Ischiropoulos, J.S. Beckman (1992) Peroxynitrite, a cloaked oxidant formed by nitric oxide and superoxide, Chem. Res. Toxicolog. 5: 834-842.
[23] S. Goldstein, J. Lind, G. Merenyi (2005) Chem. Rev. Chemistry of Peroxynitrites as Compared to Peroxynitrates, 105: 2457-2470.
[24] V.L. Lobachev, E.S. Rudakov (2006) The chemistry of peroxynitrite, Reaction mechanisms and kinetics, Russian Chemical Reviews 75(5): 422 – 444.
[25] P. Lukes, E. Dolezalova, I. Sisrova, M. Clupek (2014) Plasma Sources Sci. Technol. 23: 015019 (15pp).
[26] J.-L. Brisset, B. Benstaali, D. Moussa, J. Fanmoe, E. Njoyim-Tamungang (2011) Acidity control of plasma-chemical oxidation: applications to dye removal, urban waste abatement and microbial inactivation, Plasma Sources Sci. Technol. 20: 034021 (12 pp).
[27] Piskarev IM, Ivanova IP, Trofimova SV, Ichetkina AA and Burkhina OE (2014) Formation of Peroxynitrite Induced by Spark Plasma Radiation. High Energy Chemistry 48(3): 213-216.
[28] R. Kissner, T. Nauser, P. Bugnon, P.G. Lye and W.H. Koppenol (1997) Formation and properties of peroxynitrite as studied by laser flash photolysis, high-pressure stopped-flow technique, and pulse radiolysis, Chem. Res. Toxicol. 10: 1285-1292.
[29] Ivanova IP, Trofimova SV, Burkhina O.E., Piskarev IM. (2015) Peroxynitrite complex production under pulsed spark gas-discharge plasma radiation in air. Research Journal of Pharmaceutical, Biological and Chemical Science 6(4):1205-1219.
[30] I.P. Ivanova, I.M. Piskarev, S.V. Trofimova (2013) Comparison of biocidal and sporicidal effects of spark discharge plasma and mercury-vapor low pressure lamp radiations, IOSR J. of Pharmacy, 3(4): 51 – 55.
[31] C. Szabo, H. Ohshima (1997) DNA damage induced by peroxynitrite: subsequent biological effects, Nitric Oxide: Biology and Chemistry 1(5): 373 – 385.
[32] I.P. Ivanova, S.V. Trofimova, M.V. Vedunova, A.S. Zhabereva, M.P. Bugrova, I.M. Piskarev (2014) Assessment of cytotoxic effect mechanisms of gas-discharge plasma radiation, Sovremennye Tekhnologii v Medicine – (Modern Technologies in Medicine) 6(1): 14 – 22.